K-C_{70}: Stable phases and electronic structures

M. Knupfer,* D. M. Poirier, and J. H. Weaver
Department of Materials Science and Chemical Engineering, University of Minnesota, Minneapolis, Minnesota 55455
(Received 20 September 1993)

Photoelectron spectroscopy has been used to determine the K_xC_{70} phase diagram for $0 \leq x \leq 6$ and to investigate the electronic properties of the stable phases. Core-level analysis and vacuum distillation experiments indicate equilibrium K_1C_{70}, K_4C_{70}, and K_6C_{70} phases at 300 K. They show a eutectoid transformation from a high-temperature K_3C_{70} phase into K_1C_{70} and K_4C_{70} at 440 K. Studies in the low-doping regime demonstrate that K incorporation raises the ordering transition temperatures relative to those observed for pure C_{70}. These stabilizations are discussed in terms of peritectoid transformations. The K-C_{70} results are then examined in the context of the alkali-metal fullerides of C_{60} to obtain a broader view of the thermodynamics of both systems. Valence-band photoemission results demonstrate that the singly and doubly degenerate lowest unoccupied states of C_{70} are filled upon doping to $x=6$. They also demonstrate that none of the K-C_{70} phases are metallic, despite odd-integer filling, with band splittings that are related to reduced crystal symmetry and electron-electron correlation. Finally, the deposition of small quantities of C_{70} onto a potassium film at 40 K demonstrates that the ionization state for C_{70} molecules can be increased beyond 6.

I. INTRODUCTION

While the behavior of solid C_{60} upon doping has been investigated extensively,[1] very little is known about the compounds of C_{70}, the next stable fullerene. The maximum conductivity of K- and Rb-doped C_{70} has been observed to be more than 100 times smaller than that for the corresponding C_{60} compounds.[2,3] Photoemission studies have been reported for K-doped C_{70} by Benning *et al.*,[4] and for Rb-doped C_{70} by Takahashi *et al.*[3] The dielectric function and the distribution of unoccupied electronic states has been investigated using electron-energy-loss spectroscopy by Sohmen and Fink.[5] Imaeda *et al.*[6] have used electron-spin resonance and microwave absorption to probe the electronic and magnetic properties of K_xC_{70}. No evidence of superconductivity has been reported for alkali-metal-doped C_{70} and, to our knowledge, no reports have been presented of the stable phases of the C_{70} fullerides. While we might expect similarities to the C_{60} fullerides, we also note that fine tuning of the C_{60} fullerides by alkali-metal substitutions has resulted in a variety of intriguing properties.[1] Such subtleties should be manifest in C_{70} as well, exacerbated by the different ordering transitions of C_{70}.[7–9]

This paper focuses on the structural and electronic properties of K-doped C_{70}, starting with high quality crystalline C_{70} thin films. We have used core-level photoemission to investigate the stoichiometry- and temperature-dependent occupancy of the interstitial sites of the C_{70} lattice, deducing information concerning the phase diagram. At each stage, we have used valence-band photoemission to probe the occupied part of the electronic structure. Some aspects of these studies are analogous to those for the C_{60} fullerides where core-level photoemission provided insight into the occupation of the tetrahedral and octahedral sites and established the existence of a eutectoid transformation for $0<x<3$ at 425 K for K_xC_{60}.[10,11] Interesting perspectives are offered by distillation experiments that allowed us to probe the high-temperature behavior of the K-C_{70} system.

We find three equilibrium phases at room temperature, namely K_1C_{70}, K_4C_{70}, and K_6C_{70}. For K_1C_{70}, the K ions occupy the pseudo-octahedral sites in the close-packed C_{70} structure. K_4C_{70} and K_6C_{70} exhibit characteristics analogous to their C_{60} counterparts. The K_3C_{70} structure is stable above 440 K but transforms upon cooling into K_1C_{70}, plus K_4C_{70}, exhibiting eutectoid behavior. We propose a K-C_{70} phase diagram, compare with the C_{60} fullerides, and discuss the implications. In the low-doping regime, we find dopant-induced increases in the ordering temperatures relative to pure C_{70}. Such stabilizations are discussed in terms of peritectoid transformations.

Valence-band photoemission results confirm electron transfer to the low-lying unoccupied states of C_{70}. They also demonstrate that none of the K-C_{70} phases has states near the Fermi level. This explains the transport properties and the absence of superconductivity. We interpret the formation of band gaps in terms of the reduced symmetry of the crystal lattice and the effects of electron correlation. Finally, although electron transfer is limited to six for crystalline C_{70}, we show that the ionization state of C_{70} can be increased for C_{70} molecules "solvated" on a potassium metal surface. This tendency to accept more than six electrons suggests that higher doping is possible in the C_{70} host, as for $Na_{10}C_{60}$ (Ref. 12) and the alkaline-earth-doped fullerides Ca_5C_{60} (Refs. 13 and 14) and Ba_6C_{60}.[15,16]

II. EXPERIMENT

Most of the C_{70} films studied here were $\sim$200 Å thick, but those used for the distillation experiments were con-

siderably thicker. All were grown on GaAs(110) substrates that were cleaved *in situ*. The growth, doping, and subsequent characterizations were performed under ultrahigh vacuum conditions. C_{70} was evaporated from a tantalum boat ~10 cm from the GaAs surface. The deposition rate, 0.5–1 monolayers per minute, was monitored by a quartz-crystal oscillator. The substrate was held at ~450 K during film growth. Scanning tunneling microscopy studies[17] of C_{70} samples grown under these conditions showed a close-packed surface at room temperature with at least 400×400-Å^2 domains. Low-energy electron-diffraction measurements at 300 K showed a 1×1 hexagonal pattern, and measurements at 40 K (Ref. 18) revealed a doubling of the unit cell, as observed with electron[7] and x-ray[8,9] diffraction.

These C_{70} films were doped at ~450 K by exposure to a potassium flux from thoroughly degassed SAES getter sources. The doping concentrations were determined from K 2*p* and C 1*s* core-level intensities, taking into consideration the calculated cross sections[19] for the photoemission process. A tungsten filament was used as a heater during the growth, doping, and subsequent distillation. The distillation procedures were done by heating *in vacuo* to desorb either C_{70} or K. Core-level measurements as a function of time at temperatures of 495–650 K showed the changes in stoichiometry with stabilization when distinct phase boundaries were reached. Temperatures were determined with a chromel-alumel thermocouple attached to the sample holder. The estimated uncertainty in absolute sample temperature was ±25° for measurements done at ~425 K or above. This is a very conservative estimate that considers possible errors related to positioning of thermocouples. The reproducibility in temperature was much better, ±2 K. Cooling to 40 K was done using a closed-cycle helium refrigerator. The measurement to maximize the ionization state were performed after C_{70} was deposited on a clean K metal surface at 40 K. Under these conditions, the formation of an ordered C_{70} array was inhibited and K ions could "solvate" the C_{70} molecules.

The valence-band photoemission measurements were performed using a He lamp ($h\nu=21.2$ eV). The data were corrected for the contribution from HeI satellite radiation. Photoemitted electrons were energy analyzed with a double-pass cylindrical mirror analyzer. The energy resolution was 60 meV. High-resolution core-level studies were performed using monochromatized Al $K\alpha$ radiation ($h\nu=1486.6$ eV) with an energy resolution of 600 meV. Angle-dependent results were obtained by tilting the sample relative to the acceptance aperture of the hemispherical analyzer. Lower-resolution studies done in parallel with the valence-band investigations used nonmonochromatic Al $K\alpha$ radiation to determine stoichiometries. All spectra are referenced to the Fermi level of the grounded spectrometers, E_F.

Particular attention was paid to the possibility of "surface" effects. For $x\leq1$ and $x\geq4$, there were no differences, within experimental error, in stoichiometries deduced from x-ray photoemission measurements done with takeoff angles of 75° and 15°, although this should change the probe depth by a factor of ~4. Likewise, the emission from the C_{70} states occupied during doping scaled with the core-level results. For $1<x<4$, however, the surface-sensitive valence-band results and the grazing emission core-level results showed an apparent K deficiency relative to that deduced from the bulk sensitive measurements. The largest difference occurred at $x=3$, where the surface sensitive results gave x values that were lower by ~30%. This difference can be related to the microscopic structure of the surface itself. As we will discuss below, cycling through the eutectoid temperature for $1<x<4$ induces crystallographic transformations and phase separations. This would influence the microstructure, reducing grain sizes and introducing defects.[20,21]

III. RESULTS AND DISCUSSION

A. Phase formation at 300 K

In Fig. 1 we show a series of K 2*p* core-level spectra acquired at room temperature. For the spectrum at $x=0.4$, the background contribution from the C 1*s* satellites has been subtracted.[4] (The C 1*s* spectra are shown below.) At the lowest doping, a spin-orbit split $2p_{3/2,1/2}$ doublet appears at 295.2 and 298.0 eV. By analogy to K-C_{60},[10,11] this doublet can be attributed to K ions in

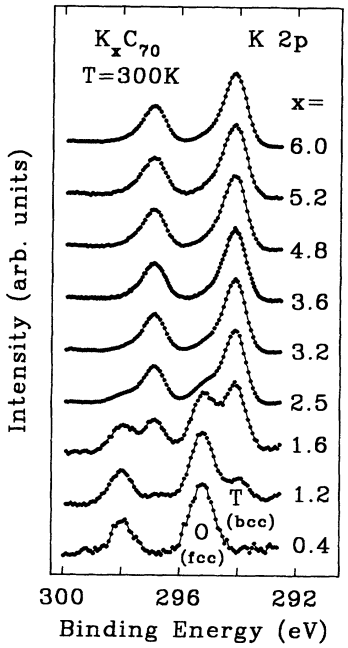

FIG. 1. K 2*p* core-level spectra for K_xC_{70}, measured at 300 K and normalized in height. Doping first results in K ions in pseudo-octahedral sites of the fcc-based C_{70} lattice, labeled *O*, as K_1C_{70} forms with $2p_{1/2,3/2}$ features at 298.0 and 295.2 eV, respectively. A second doublet, labeled *T*, develops at the expense of the first when x exceeds 1 because a bcc-based K_4C_{70} nucleates and grows. For x between ~1 and ~4, the spectra represent a superposition of the two phases in a ratio corresponding to the lever rule. Doping beyond 4 gives rise to K interstitials in the K_4C_{70} lattice, and ultimately to K_6C_{70} formation.

pseudo-octahedral sites of the close-packed C_{70} lattice. This analogy is justified by the likelihood that the Madelung potentials of these sites are comparable to those of C_{60} and the two fullerenes have approximately equal polarizabilities. These sites have lower symmetry than in C_{60} because of the lower symmetry of the C_{70} molecules themselves,[22] and are "pseudo-octahedral." The K binding energies are slightly higher than in C_{60} because of the larger lattice constant.[8,9] This interstitial site filling should be independent of whether the starting phase of C_{70} had face-centered-cubic (fcc) or hexagonal-closed-packed (hcp) symmetry[8,9] at the growth temperature because pseudo-octahedral sites are present and, in terms of their first coordination shell with C_{70}, they are identical in both structures. From geometric considerations, the octahedral site diameter is 2.07 Å at room temperature based on the lattice constant and the molecular orientation.[8,9]

The exclusive filling of octahedral sites for $x \leq 1$ implies that a K_1C_{70} phase is formed at room temperature. This structure is analogous to the Rb_1C_{60} and Cs_1C_{60} phases at 300 K,[10] as well as Cs_1C_{84}.[23] It is also analogous to the K_1C_{60} phase that is an equilibrium phase only above 425 K.[11]

A second K 2*p* doublet develops at 294.1 and 297.0 eV when x exceeds 1, as pseudotetrahedral site occupancy becomes necessary. Figure 1 shows that this tetrahedral feature grows while emission from the octahedral site decreases. Emission from the octahedral sites is lost by $x \sim 4$. This behavior is very different from what has been observed in either K-C_{60} or K-C_{84} at 300 K (Refs. 10, 11, and 23) because both had $x=3$ phases that nucleated after the terminal solubility of the solid solution phase was exceeded. In those cases, there was a fixed ratio of ~2:1 in the emission intensities for ions in the tetrahedral and octahedral sites for $0 < x \leq 3$ because the $x=3$ phase was fcc derived.[10,11,23] Further analysis of Fig. 1 indicates that the energy difference between the "octahedral" and "tetrahedral" features is smaller than observed for K_3C_{60}.[10] Instead, it agrees with the difference observed for K ions in octahedral sites of K_1C_{60} and tetrahedral sites of K_4C_{60}.[10,11] We conclude that doping beyond $x=1$ at 300 K results in the formation of K_4C_{70} with a body-centered-derived structure.[24] The K-C_{70} results are analogous to what was seen in Cs-C_{60}, a system characterized by the formation of Cs_1C_{60} and Cs_4C_{60} and the absence of an $x=3$ phase at room temperature.[10]

Figure 2 presents a provisional phase diagram for the *K-C*$_{70}$ system. Although photoemission is a surface-sensitive technique, the x-ray photoemission spectroscopy (XPS) results presented here for the K 2*p* and C 1*s* photoelectrons cover a probe depth of ~75 Å. Previous XPS results for C_{60} fullerides have been consistent with bulk structural data.[4,10] For K-C_{60}, those results were used to demonstrate the existence of a eutectoid transformation involving bulk K_1C_{60}, K_3C_{60}, and solid solution phases.[11] The above discussion of the K 2*p* core-level results allows us to establish much of the behavior at 300 K. Other portions are deduced from results presented below. At

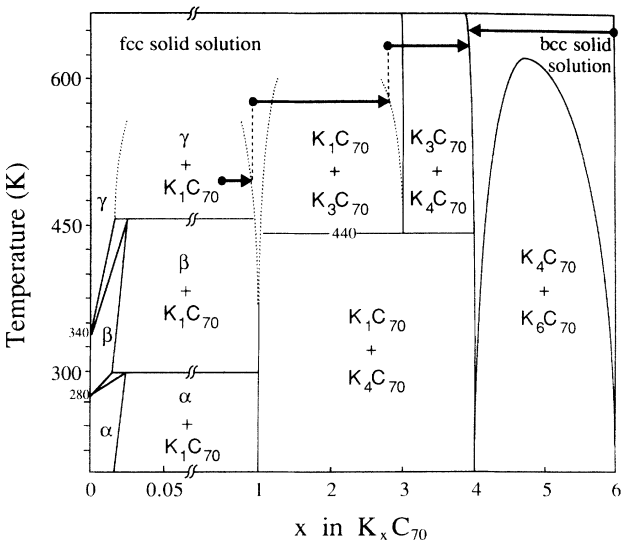

FIG. 2. Provisional phase diagram of K-C_{70} based on the results presented here for K incorporation and values from the literature for the transformation temperatures between the aligned-and-frozen, aligned-but-rotating, and tumbling phases. Dilute doping stabilizes these ordered phases, raising their transition temperatures and defining the α, β, and γ-solid solution fields. These fields are shown to terminate at classical peritectoid transformations, although the exact stoichiometries and temperatures are not known. At higher doping levels, there is coexistence with K_1C_{70}. For $x > 1$, the phase diagram shows separation into K_1C_{70} and K_4C_{70} below a eutectoid temperature of 440 K and the formation of K_3C_{70} above 440 K. The implications of this $K_3C_{70} \rightleftarrows K_1C_{70} + K_4C_{70}$ transformation are discussed in the text. Doping beyond about 4 produces another two-phase region, the character of which depends on temperature. A high ordering tendency of the K ions in the tetrahedral sites would raise the miscibility gap. The horizontal arrows depict distillation pathways with terminal stoichiometries determined from core-level intensities.

300 K, we conclude that K_1C_{70} and K_4C_{70} are the equilibrium phases. For $1 < x < 4$, there will be coexistence with the relative amounts of the phases dictated by equilibrium thermodynamics. Accordingly, the spectral results of Fig. 1 represent the superposition of contributions from those phases for $1 < x < 4$. This is consistent with the observation that the two K 2*p* doublets in Fig. 1 have equal intensities at $x = 1.6$, as required by the lever rule at this doping level. Indeed, fitting of the core-level spectra throughout this range supports this equilibrium picture.

Figure 1 shows that there were no changes in spectral shape in the K 2*p* spectra for doping beyond $x=4$, as for K-C_{60} where all of the ions were in tetrahedral sites in the bcc-based lattice for $x > 4$.[10] Doping beyond $x=6$ resulted in the accumulation of a surface species with potassium-oxygen bonding, as was evident from the appearance of O 1*s* core-level emission. Under such conditions, x-ray photoemission measurements at grazing emission showed a buildup of K on the surface, bonded to oxygen. No surface excess was evident in angle-dependent studies at lower stoichiometry.

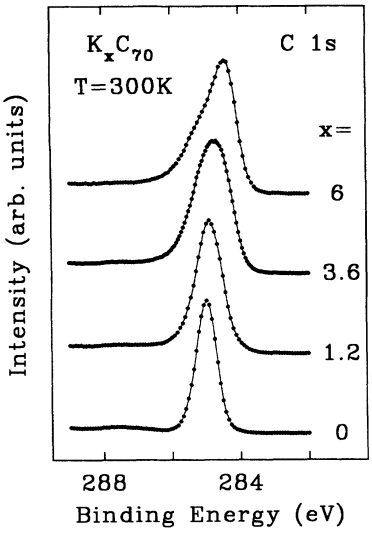

FIG. 3. Normalized C 1*s* photoemission spectra for K_xC_{70}. The spectrum for $x=0$ represents pure C_{70} at 300 K with a binding energy of 285 eV and a full width that suggests almost equivalent C sites. The spectrum for $x=1.2$ represents the K_1C_{70} phase with broadening due to inequivalent C atoms because of the filling of the pseudo-octahedral sites. For $x=3.6$, a nearly pure K_4C_{70} sample, the C 1*s* core level is slightly shifted to lower binding energies and considerably broadened. Doping beyond $x=4$ produces an asymmetric C 1*s* spectrum that suggests a reduced symmetry for the K_6C_{70} phase.

Additional information can be obtained by considering the C 1*s* core-level spectra of Fig. 3. The spectrum for undoped C_{70} is shown at the bottom with a full width at half maximum of 0.7 eV and centered at 285-eV binding energy. Doping to about $x=1$ led to a peak shift to 284.9 eV and a broadening (width ~ 1.0 eV). The lower binding energy reflects the change due to the adjacent K^+ ions and the screening of C 1*s* holes by the additional electron on the C_{70} molecule in K_1C_{70}. The larger width indicates that the C atoms become more inequivalent due to the filling of the pseudo-octahedral sites. Doping beyond $x=1$ resulted in a slight shift in binding energy and considerable broadening (~ 1.3 eV at $x=3.6$, a sample that would be $\sim 90\%$ K_4C_{70}). The C 1*s* level was markedly asymmetric for $x>4$, suggesting reduced lattice symmetry for the K_6C_{70} phase. It must remain for diffraction analyses to determine the symmetries of the phases, but the spectroscopic evidence demonstrates their stoichiometries.

B. Temperature dependencies and a eutectoid transformation

Core-level photoemission studies conducted as a function of temperature and composition for $1 \leq x \leq 4$ make it possible to determine changes in site occupancy for the K ions. In this way, it is possible to demonstrate phase transformations, as was done by Poirier and Weaver[11] for K-C_{60}. Their work showed an invariant transformation, written $K_1C_{60} \rightleftarrows C_{60}$(solid solution)$+K_3C_{60}$, where the eutectoid temperature was 425 K, in agreement with temperature-dependent Raman spectroscopy studies of K_xC_{60} (Ref. 25) and reanalysis of x-ray data.[26,27] Here, K_3C_{70} was not stable at 300 K, but we suspected that it might be stable at higher temperature.

Figure 4 shows K 2*p* core-level results for $K_{2.5}C_{70}$ obtained at 300 and 450 K. The lower-temperature results are characteristic of K_1C_{70} and K_4C_{70} in a ratio of 1:1 for $K_{2.5}C_{70}$. Line-shape decomposition shows that the intensity ratio between tetrahedral and octahedral features was ~ 4 at 300 K, with tetrahedral emission representing ions in bcc-based K_4C_{70}, and octahedral emission corresponding to fcc-based K_1C_{70}. Heating to 450 K changed the tetrahedral-to-octahedral ratio to ~ 1.5 and shifted the energy position of the tetrahedral feature to that expected for a fcc-based structure.[10] We note that a change due to lattice expansion would lead to a shift in the opposite direction. Heating to higher temperatures had no effect beyond thermal broadening and, ultimately, distillation (discussed below). Cooling to 300 K restored the signature shown. Measurements for samples of lower or higher stoichiometry produced analogous behaviors, with differences related to the relative amounts of the phases present. For a sample with x very near 3 obtained by distillation, the low-temperature structure was again two phase, but high-temperature results showed a tetrahedral-to-octahedral ratio of nearly 2, the value expected for ions distributed in an A_3C_{60}-like lattice. Together, these results demonstrate that there is a eutectoid reaction that dictates the transformation from one phase (K_3C_{70}) into two ($K_1C_{70}+K_4C_{70}$) upon cooling through the invariant temperature of 440 K, as depicted in Fig. 2.

We propose that K_3C_{70} is unstable at low temperature because the pseudotetrahedral sites are reduced in size by the alignment of the C_{70} molecules. In particular, the "top" molecule of a C_{70} tetrahedron would be directed toward this interstitial site. This could lead to a higher formation energy for a fcc-type K_3C_{70} structure compared to a bct-like K_4C_{70} structure. Above 440 K,

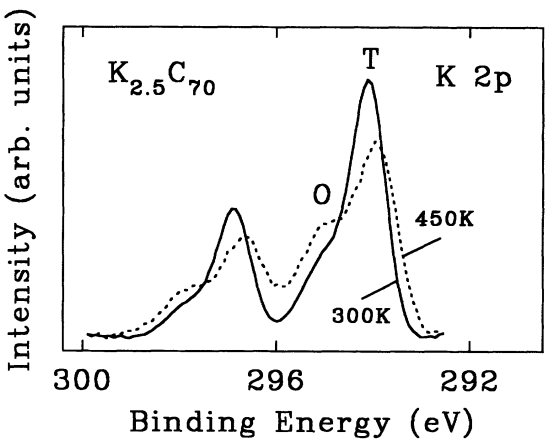

FIG. 4. K 2*p* core-level spectra for $K_{2.5}C_{70}$ measured at 300 and 450 K. These results, which are representative of those for $1<x<4$, show a transformation from a K_3C_{70} phase (with tetrahedral and octahedral site occupancy in the fcc-based lattice with a 2 to 1 ratio) to a mixed-phase regime, $K_1C_{70}+K_4C_{70}$, upon cooling. The binding energies for the K ions are distinctly different in the fcc- and bcc-based structures.

thermally activated libration of C_{70} molecules may lead to a structure that has an averaged fcc symmetry with the tetrahedral sites enlarged compared to lower temperatures. This might favor the formation of K_3C_{70}, as in K_3C_{60} and K_3C_{84}.[10,11,13]

C. Distillation studies

Distillation studies that involve heat treatments and preferential desorption make it possible to obtain isothermal cuts across the phase diagram. Isothermal distillation takes advantage of the difference in vapor pressure for the components of a single-phase sample or the difference in vapor pressure for the two phases in a coexistence region. Although complex to model on an atomic or molecular scale, fulleride distillation proceeds until a single phase is reached that is stable.[28] Here, distillation experiments for K-C_{70} allow us to confirm the formation of K_1C_{70}, K_3C_{70}, and K_4C_{70}, and to identify some of the high-temperature phase boundaries.

Figure 5 shows the results of distillation experiments for K_xC_{70}. The data points represent measured compositions as a function of time at the temperatures indicated. The lines were added as a guide to the eye. The bottom curve shows the changes in composition of an 800-Å-thick film that had an initial stoichiometry of $K_{0.5}C_{70}$ as it was held at 495 K *in vacuo*, then 575 K, and finally 635 K. The measured compositions at saturation are close to K_1C_{70}, K_3C_{70}, and K_4C_{70}. The corresponding distillation pathways are indicated by the arrows in Fig. 2. We emphasize that the final compositions represent phase boundaries at the given distillation temperatures, as depicted by the points of the arrows in Fig. 2. An end point of distillation can deviate substantially from an integer value at high temperature because it represents the thermodynamic state with the lowest free energy. Since the vacancy energy is small, this can be well away from the integer stoichiometery for an open thermodynamic system such as that represented by the distillation experiment. Once equilibrated, the films were stable against further changes at the distillation temperatures.

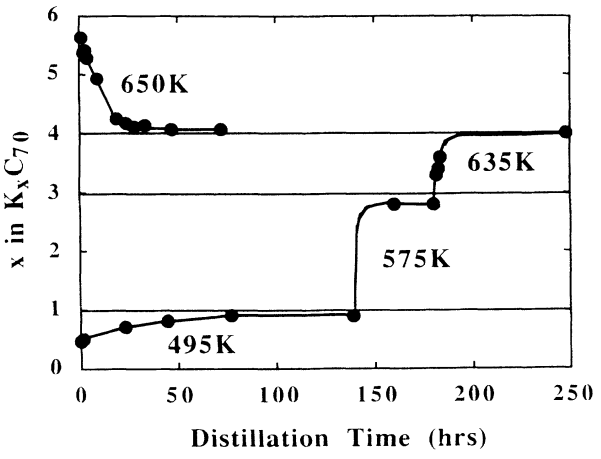

FIG. 5. Summary of results obtained during distillation of samples of initial stoichiometry of $K_{0.5}C_{70}$ and K_6C_{70} at the temperatures given. These distillation pathways are drawn as isothermal lines in Fig. 2. For $x<4$, distillation favors C_{70} sublimation until stable phase boundaries are encountered. Such behavior leads to K_1C_{70}, K_3C_{70}, and K_4C_{70} with stoichiometry deviations that reflect the stable phase in an open thermodynamic system at the appropriate temperature. Distillation from $x=6$ also terminates at $x\cong 4$ because K_4C_{70} is the most stable phase.

In Fig. 5, the increase in relative K content indicates that C_{70} evaporates when the stoichiometry is below ~ 4. In contrast, the relative K content can be reduced by distillation of a saturated K_6C_{70} film. In this case, heating to 650 K produces K_4C_{70}, as seen in the top curve. The fact that K_4C_{70} is reached by distilling from either higher or lower stoichiometry indicates that this compound is the most stable in the K-C_{70} series against sublimation. Even K_4C_{70} can also be sublimed, but this occurs stoichiometrically; at 675 K the sublimation rate is ~ 0.2 monolayers per hour.

Figure 2 depicts K_4C_{70} and K_6C_{70} as phases that can tolerate appreciable deviations from stoichiometry. At high temperature, above a miscibility gap, the phases merge and the tetrahedral sites would be occupied randomly. Since the width of the miscibility gap reflects the details of the ion-ion interactions, it would extend to relatively high temperature if K_4C_{70} and K_6C_{70} were well ordered. (In the limit of high ordering, the system would exhibit a different behavior. At high temperature, it would form a liquid and the liquid would transform into solids via eutectic or peritectic reactions. In our picture, we are assuming that the $x=4$ phase undergoes a change in lattice constant upon doping and ultimately is indistinguishable from an $x=6$ phase with a large number of vacancies.) If the enthalpies of formation of these phases are nearly equal, as calculations have suggested for K-C_{60},[29] and they are close to the enthalpies of a random array of K ions in the interstitial sites, then a miscibility gap would be much lower. While we cannot define the top of the miscibility gap with precision, the distillation experiments at 650 and 635 K from higher and lower stoichiometries resulted in single-phase K_4C_{60}. This supports placement of the miscibility gap below ~ 635 K; if it were above, one might expect two different distillation end points, terminating on the two extremes of the K_4C_{70} phase field.

D. Solid solutions and orientational ordering

Equilibrium doping of C_{70} first produces a solid solution of K ions in the lattice, favoring octahedral sites. This is analogous to K-C_{60}, where we termed the solid solution the α phase and did not distinguish between solid solutions of the simple cubic phase and the fcc phase.[10] The differences in solution for these two phases have not yet been explored for C_{60}, but one can anticipate that the first-order transition from simple cubic (sc) to fcc pure C_{60} must be extended to a peritectoid reaction upon doping, and coexistence fields must be established. Indeed, Samara *et al.*[30] have found that the sc structure could be stabilized by hydrostatic pressure, finding an increase in transition temperature of ~ 90 K under 8 kbar of pressure. For C_{70}, with a close-packed phase above

~340 K, a rhombohedral or distorted hcp phase between ~280 and ~340 K, and a monoclinic phase below ~280 K,[8,9] there must be three solid solution phases and, assuming that the transformations are first order, there must be two invariant reactions and two regions of coexistence. Since K or other impurities in the C_{70} lattice should hinder rotation and tumbling, the ordered phases should be stabilized.

To investigate phase stabilization, we undertook valence-band photoemission studies of pure C_{70} and K-doped C_{70} in the dilute regime. They were motivated by the fact that Knupfer, Poirier, and Weaver[18] recently demonstrated that the electronic structure, and hence the photoemission spectra, were sensitive to molecular ordering. Figure 6 summarizes the results for a sample of stoichiometry $x \cong 0.05$ measured at 40, 300, and 450 K. The inset compares the spectra for undoped and doped C_{70} at 450 K. For undoped C_{70}, there are distinct features at 2, 2.6, 2.9, 3.5, and 4.2 eV. Upon doping, Fig. 6 demonstrates that they shift uniformly ~0.3 eV to higher binding energy as the Fermi level is pinned at the edge of the lowest unoccupied electronic states, as for K_xC_{60}.[4,31] The group of levels within ~3 eV of E_F accounts for 20 electrons, and the group between ~3 and ~5 eV accounts for another 20. These occupied states are derived from nondegenerate or twofold degenerate molecular orbitals with π character, as discussed by Andreoni, Gygi, and Parrinello.[32] For undoped C_{70}, cooling from the high-temperature random-tumbling phase to the aligned-but-rotating and then the aligned-but-frozen phases resulted in spectral differences that were particularly evident in the feature near 3.5 eV (~3.8 eV in Fig. 6 because of the Fermi-level shift) and the shoulder-peak-shoulder appearance of the leading manifold of states. The 3.5-eV feature was sharpest for the random-tumbling phase, and least distinct in the ordered low-temperature phase.[18]

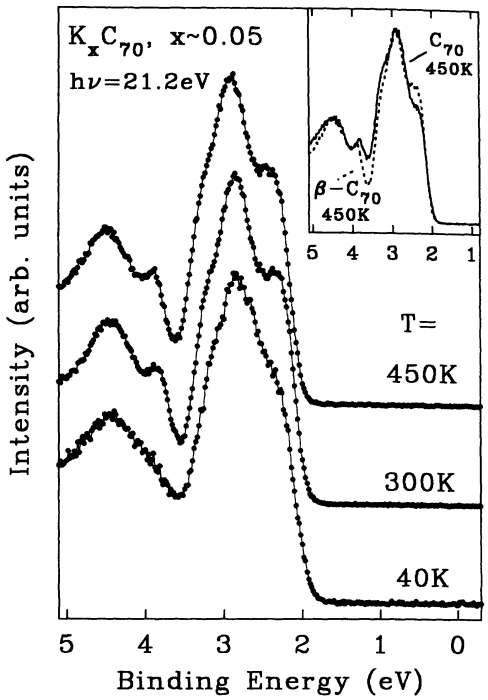

FIG. 6. Valence-band photoemission spectra for dilute doping of C_{70} with $x \cong 0.05$. The low-temperature spectrum is indistinguishable from that of pure C_{70}. The results obtained at 300 and 450 K show changes in the ~3.8- eV feature and the shoulder-peak-shoulder line shapes because of the transformation from the low-temperature phase into the high-temperature phase characterized by molecular rotation. The inset shows that spectrum for the stabilized β-C_{70} phase differs substantially from that of pure C_{70} at 450 K, i.e., from the random-tumbling state.

Comparison of the doped and undoped results at 40 K revealed identical behavior, as expected because the temperature was far below the ordering temperature of the host. However, examination of the doped results at 300 and 450 K shows no changes other than phonon broadening, in contrast to what is found for undoped C_{70}.[18] In the inset of Fig. 6 we compare the doped and undoped results measured at 450 K. (The spectrum for pure C_{70} is shifted to compensate for the Fermi-level shift.) The two curves differ sharply, especially at ~2.3 and ~3.8 eV. This indicates that the ordering of the C_{70} molecules is different in the two samples. Moreover, the curve for the slightly doped sample at 450 K is nearly identical to that of pure C_{70} at room temperature.[18] We conclude that dilute doping of C_{70} stabilizes the aligned-but-rotating phase to at least 450 K, preventing the molecules from undergoing random tumbling. Modest doping of C_{70} then has a comparable effect as modest hydrostatic pressure for C_{60} (Ref. 30) with respect to the tumbling transition. Unfortunately, heating above ~450 K resulted in distillation and prevented further investigation.

To take into account the three distinct phases for pure C_{70} and the stabilization induced by dilute doping, in Fig. 2 we sketch a provisional low x-phase behavior that is consistent with elementary first-order thermodynamics. The transitions for pure C_{70} are taken to occur at 280 and 340 K, but these temperatures represent averages from the literature[7–9] and may be refined. Solid solutions formed from the three pure phases are labeled α, β, and γ. The transition temperatures will increase with doping until the solubility limits are reached. The β-γ transition occurs above ~450 K at the solubility limit, as denoted by the horizontal line at about 455 K. The peritectoid transformation from γ-C_{70} plus K_1C_{70} into β-C_{70} then necessitates coexistence fields, as sketched, although the positions of the phase boundaries remain to be determined. For the α-β transition, we expect a corresponding increase in temperature upon doping, but the data indicate that it remains below room temperature at the solubility limit. The fact that the β-γ transition is stabilized more than the α-β transition is consistent with the expectation that free tumbling of a "rugby ball" in a lattice is more easily frustrated than spinning. Pressure-dependent studies of pure C_{70} and further dopant-dependent investigations are clearly needed. As a caution, we note that unintentional "doping" with impurities is likely to raise the transition temperatures.

E. Comparisons of K_xC_{70} with A_nC_{60}

The phase diagram of Fig. 2 indicates that doping beyond the terminal solid solubilities for α, β, and γ

phases will nucleate the K_1C_{70} phase. Doping beyond $x=1$ below 440 K will result in K_4C_{70} nucleation and coexistence with K_1C_{70}. Doping between $x=1$ and 3 above 440 K will produce K_3C_{70} with no K_4C_{70} formation until x exceeds 3. Finally, K_6C_{70} will be formed and saturation doping will be achieved at $x=6$. While the proposed phase diagram specifies stoichiometries, it does not contain the details of the various crystal structures. In particular, the crystal symmetry of the phases might be lower than the respective K_xC_{60} phases since C_{70} itself has a lower molecular symmetry. Such structural detail must await diffraction experiments.

The differences in the K-C_{60} and K-C_{70} phase behaviors can be examined through Fig. 7, where we depict very schematically the Gibbs free energies G as a function of stoichiometry for the phases that have been reported. The phase diagram represents a collection of such sketches, each obtained at a different temperature. K_4C_{70} is always the most stable, and G is drawn accordingly. Coexistence of K_4C_{70} and K_6C_{70} is reflected by the tie line for $x=4$ and 6. At the left, the solid solution phases are depicted as a single curve, although there should be separate curves for the α, β, and γ solutions. The relative values for the minima in G for K_1C_{70} and K_3C_{70} depend on temperature. Below 440 K, the free-energy minimum for K_3C_{70} falls above the tangent line drawn between K_1C_{70} and K_4C_{70}, and it is unstable. Above 440 K, G lies lower and new tangent lines that intersect K_3C_{70} must be included, as drawn by dashed lines. Three phases will coexist when a common tangent line can be drawn and conditions are established for a eutectoid ($x=1,3,4$) or peritectoid ($\alpha,\beta,1$ or $\beta,\gamma,1$) reaction.

Studies of the fullerides of C_{60}, and now C_{70}, have shown that changes in the host-guest pairing alter the relative stabilities of the A_1C_n and A_3C_n phases for $A=$K, Rb, and Cs, as can be understood from the free-energy sketches in Fig. 7. For example, K_1C_{60} is stable above 425 K, an effect related to rotation of the fullerenes that reduces the size of the tetrahedral sites so that K_3C_{60} is then destabilized relative to K_1C_{60} for $0<x\leq 1$. Replacing K by a larger ion, Rb, stabilizes the A_1C_{60} phase at all temperatures for $x\leq 1$. Substituting Cs for K destabilizes the A_3C_{60} phase altogether, giving a phase diagram at 300 K that is similar to Fig. 2. It remains to be seen whether Cs_3C_{60} is stable at elevated temperature, but we speculate that it is. We also speculate that substitution of Rb or Cs for K in C_{70} will produce $x=1$ phases and will raise the eutectoid temperature above 440 K.

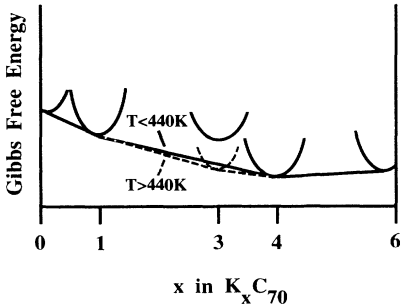

FIG. 7. Schematic plots of the Gibbs free energies for the solid solution phase and the K_1C_{70}, K_3C_{70}, K_4C_{70}, and K_6C_{70} phases. Thermodynamic considerations stipulate that phases connected by tie lines, as drawn, will coexist for intermediate stoichiometries. For the temperatures associated with the solid lines, these correspond to $\alpha+1$, $1+4$, and $4+6$. Changes in temperature shift the free-energy curves. The dashed lines depict conditions under which K_3C_{70} is stable, as is the case when $T>440$ K (Fig. 2).

Finally, we note that the eutectoid reaction that links (bcc-based) K_4C_{70} to (fcc-based) K_1C_{70} and (fcc-based) K_3C_{70} will be sluggish because the change in crystal structure introduces a free-energy barrier against nucleation of the nascent phase. Accordingly, one must be careful to avoid quenching in the high-temperature phase, and should be aware of the implications of cycling through the eutectoid temperature as far as the microstructure is concerned.[20] Both effects will be important in analyzing diffraction data, particularly for powder samples.

F. Fulleride metallicity

Figure 8 shows photoemission valence-band spectra for K_xC_{70} measured at 450 K, so as to examine the propensity of each fulleride phase, including K_3C_{70}, to exhibit emission from states at the Fermi level. This would be a

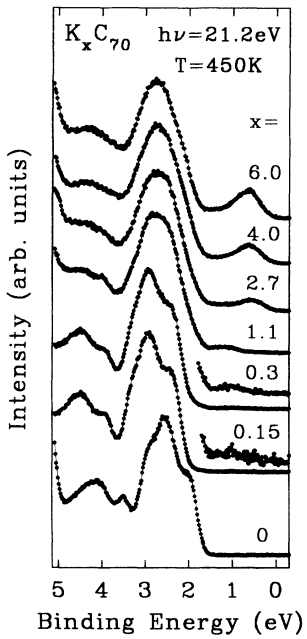

FIG. 8. Photoemission valence-band spectra for K_xC_{70} at 450 K, a temperature that stabilizes $x=1$, 3, 4, and 6 phases. The initial shift observed upon dilute doping corresponds to Fermi-level pinning at the conduction-band minimum (transport band gap 2.1 eV). Dilute doping also stabilizes the aligned-but-rotating β phase at this temperature. The spectrum for $x=1.1$ shows that the K_1C_{70} phase has a gap of at least 0.7 eV, and with a LUMO-derived feature centered 1.3 eV below E_F. The gap is related to reduced crystal symmetry and the effects of electron correlation. A gap is also observed for $x\cong 3$ but it is small. The fullerides with $x=4$ and 6 also show no emission at E_F.

necessary, but not sufficient, condition for metallic character. The bottom curve represents the high-temperature phase of pure C_{70}. As discussed above, dilute doping stabilizes the aligned-but-rotating β phase and shifts the valence bands by ~ 0.3 eV as E_F is pinned at the conduction-band minimum. The energy separation between the valence-band maximum, taken as the onset of emission, and the pinned Fermi level represents the band gap of C_{70}. This energy, 2.1 eV, is in excellent agreement with that deduced from combined photoemission and inverse photoemission experiments.[4] It corresponds to the energy needed to create an isolated electron and an isolated hole, corresponding to $N-1$ and $N+1$ final states of the molecular solid with account taken of the effects of electron correlation. Knupfer, Poirier, and Weaver[18] have shown that the electron correlation energy U for C_{70} is ~ 1 eV. Correlation effects in C_{60} have been discussed by several authors.[33–36] The transport gap exceeds the optical gap[37] because the low-energy optical transitions create electron-hole pairs that are bound on a molecule as an exciton.

The spectrum for $x=1.1$ represents the valence band of K_1C_{70}, although with a small amount of K_3C_{70}. For it, the main feature centered at ~ 2.7 eV and the feature at ~ 4.5 eV are broader than in pristine C_{70}. Cooling to 300 and to 40 K produced slightly sharper structures, but there were no other effects. Significantly, the onset of the leading feature of K_1C_{70} is 0.7 eV below E_F. This feature, centered at ~ 1.3 eV, is K induced and reflects states derived from the lowest unoccupied molecular orbital (LUMO) of C_{70}, a singly degenerate a_1'' orbital.[32] Similar placement of the first alkali-metal-induced valence-band feature has been reported in Refs. 3 and 4. Its energy position is remarkable because, in an independent particle picture, a system with one valence electron in a primitive unit cell should have a half-filled band that is cut by the Fermi level.

We propose that the width of the LUMO-derived band for K_1C_{70} and the ~ 0.7-eV gap reflect a combination of two factors, namely band splitting due to reduced crystal lattice symmetry, and electron-electron correlation. For band splitting to be important, one must consider a noncubic structure of K_1C_{70}, the likelihood of an expanded unit cell, and the folding back of the Brillouin zone. Such symmetry lowering would not be surprising given the oblong shape of C_{70} and the doubling of the unit cell observed for C_{70} at low temperature.[7–9] For correlation to be important, the on-site correlation energy for K_1C_{70} must be non-negligible, an effect that is reasonable given that $U \sim 1$ eV for C_{70}.[18]

Figure 9 compares the emission features near E_F for K_1C_{70} and the more symmetric isoelectronic Rb_1C_{60} compound. For Rb_1C_{60}, independent particle band calculations (rocksalt structures) predict a narrow occupied band[38] (full width <0.2 eV), while experiment[34] shows the band to be much larger. As discussed by Benning, Stepniak, and Weaver,[34] the broadening reflects electron correlation. Stepniak *et al.*[35] noted that the temperature dependence of the resistivity for Rb_1C_{60} indicates activated transport, implying localization of the states at E_F.

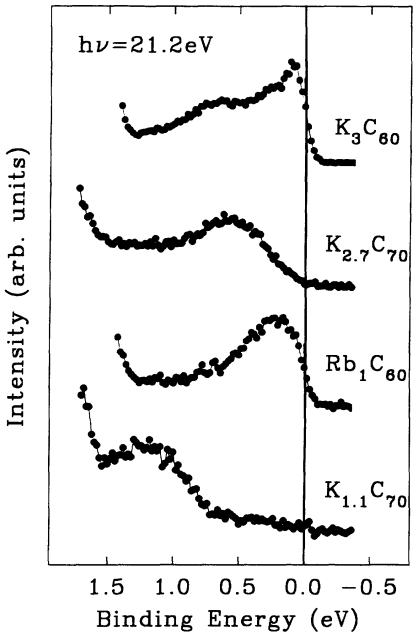

FIG. 9. Comparison of photoemission spectra for $K_{1.1}C_{70}$ and Rb_1C_{60}. In $K_{1.1}C_{70}$ there is a contribution of the K_3C_{70} phase between E_F and 0.7 eV. K_1C_{70} is insulating, despite integer filling, because of a contribution of reduced symmetry of the lattice and electron correlation. In contrast, Rb_1C_{60} shows states at E_F but with pronounced broadening of the partially occupied LUMO band. $K_{2.7}C_{70}$ exhibits a broad band of emission centered at ~ 0.5 eV with the Fermi level at the band edge. This suggests that K_3C_{70} is a narrow-gap material. In contrast, K_3C_{60} exhibits emission at E_F.

Benning, Stepniak, and Weaver[34] suggested that the location of the peak in the LUMO band well below E_F for Rb_1C_{60} was consistent with a pseudogap. With increased U relative to the bandwidth, this gap would become larger and a Mott-Hubbard-like splitting would be observed. For K_1C_{70}, we see that the LUMO band centered at ~ 1.3 eV is again very broad, suggestive of electron correlation. (In Fig. 9, there is also weak emission between this band and E_F because the stoichiometry exceeded 1, and K_3C_{70} was beginning to form.) While it is tempting to attribute the full development of a gap to Mott-Hubbard behavior, the size of the gap, 0.7 eV, is very large compared to U. This suggests that the K_1C_{70} phase has a ground-state gap because of reduction in the symmetry of the crystal lattice, and the gap measured with photoemission is increased by electron removal for a correlated system.

The spectrum in Fig. 8 for $x=2.7$ at 450 K represents the valence band of K_3C_{70}. Significantly, an additional feature due to occupation of the LUMO+1 band appears at ~ 0.5 eV, and this is emphasized in Fig. 9. Despite odd-integer doping, we again find no evidence of emission at the Fermi level. Comparison to the spectrum for K_3C_{60} (Fig. 9) shows important differences. For the latter, there is a distinct peak at E_F and there is structure at ~ 0.3 eV that has been attributed to vibronic coupling

during electron excitation. The broad feature at ~0.7 eV has been related by Benning *et al.*[36] to the incoherent part of the spectral function, and by Knupfer *et al.*[39] to coupling to an intrinsic charge-carrier plasmon during electron excitation. For K_3C_{70}, E_F lies at the edge of the band derived from the LUMO+1 orbital. The LUMO+1 band is very broad, comparable to K_3C_{60}, an effect we again attribute to correlation. The difference is that K_3C_{70} is not metallic, though the gap appears to be small. Again, the formation of the gap probably reflects a continuation of Mott-Hubbard-like behavior and the reduced symmetry of the crystal lattice.

The valence-band spectrum of K_4C_{70} exhibits a single K-induced band that is centered 0.7 eV below E_F (Fig. 8). The insulating character is analogous to what has been seen for all of the A_4C_{60} fullerides where deviations from metallic character were attributed to electron correlation and the formation of Mott-Hubbard-like insulators.[34,36] Figure 8 shows that continued doping to $x=6$ increases the intensity of the LUMO feature without introducing new features, as for the C_{60} fullerides.[4,31,34,36] A spectral shift away from E_F is generally observed in photoemission spectra as an alkali-metal fulleride is saturated to produce $x=6$. This results from a complete filling of the LUMO-derived bands and the movement of the Fermi level from the top of this band to the bottom of the LUMO+1 band. For K_6C_{70}, it was found that minimal annealing time at 450 K (the doping temperature) prevented this shift from occurring because K was desorbed. Thus the spectra in Figs. 1, 3, and 8 actually represent stoichiometries slightly less than 6.0. A shift as shown in Ref. 4 can be produced by doping at lower temperature or by cooling to room temperature immediately after doping to saturation. The insulating character of K_6C_{70} is expected since the e_1''- and a_1''-derived bands are filled. For K_6C_{70}, the centers of the highest occupied molecular orbital (HOMO) and LUMO bands are separated by ~2 eV, whereas photoemission and inverse photoemission measurements for C_{70} indicate a center-to-center separation of ~3.6 eV. Benning *et al.*[36] have discussed this effect by noting that the occupied states of the pure material are measured by electron removal, and empty states are studied by electron addition, creating $N-1$ and $N+1$ final states. For photoemission from K_6C_{70}, the LUMO is occupied and can be studied by electron removal. The effect of correlation is then obvious when the final-state configurations are different.

The results of Fig. 8 were obtained at 450 K. Cooling to 300 and to 40 K failed to give any evidence of the onset of "metallic" character or increased emission near E_F. Finally, comparison of the present data with those in the literature for K-C_{70} (Ref. 4) and Rb-C_{70} (Ref. 3) shows qualitative agreement with account taken of differences in the x values and the placement of the Fermi level. We note that the stoichiometries have been determined in previous studies by comparing the intensities of the HOMO and LUMO features, assuming constant photoionization cross sections,[4] or by thickness monitor readings during deposition.[3] Both methods are less accurate than direct measurements of the core-level intensities and binding energies. Electron-energy-loss studies of Rb_xC_{70} also found that none of the phases between $0 \le x \le 6$ is metallic.[5] The metallic K_4C_{70} phase deduced from electron-spin-resonance investigations[6] can probably be explained by a small contamination of the samples with C_{60} (and K_3C_{60}), as mentioned in Ref. 6.

G. Charge transfer to single molecules

For solid K-C_{70}, saturation occurs at $x=6$. This saturation of charge transfer need not be intrinsic to the molecule but could reflect maximum filling of the interstitial lattice sites. Previously, we have investigated higher coordination of ions with C_{60} by depositing onto an alkali-metal surface at 40 K. Under those conditions, we found partial filling of the t_{1g} band of C_{60} as a charge state of 8^- was achieved.[34] Figure 10 shows the result of equivalent C_{70} deposition onto K metal, with comparison to saturated K_6C_{70}. The spectra are normalized to the intensity of the feature located near 2.8 eV. The intensity between 0 and ~1.9 eV is much higher for C_{70} deposition onto K, and there is a significant change in line shape with an additional feature appearing at ~0.3 eV. These results indicate the filling of additional unoccupied states of C_{70}. Moreover, the ~2.8 eV feature is narrower for C_{70} on K and is shifted slightly to higher binding energy. The different shifts indicate that further electron transfer to C_{70} causes a rearrangement of the electronic structure. Adding more C_{70} ultimately results in a photoemission spectrum equivalent to K_6C_{70} as the coordination number is progressively diluted in this metastable structure.

We can estimate the K-C_{70} coordination by assuming equal photoionization cross sections for the a_1'', e_1'', and additional states. Comparison of intensities within 1.9 eV of E_F yields an effective charge transfer of ~12 electrons to the C_{70} molecules on K metal. We envision this

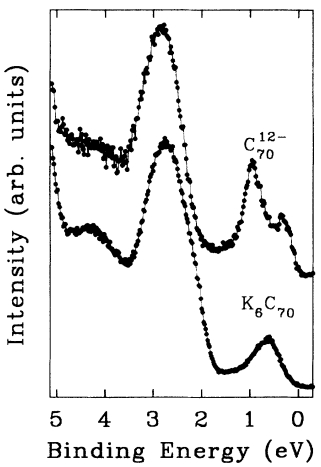

FIG. 10. Comparison of the photoemission spectrum for K_6C_{70} and for C_{70} deposited on a potassium metal surface at 40 K. The higher intensity of the leading feature and the shift to higher binding energies for the upper curve shows that more than six electrons have been transferred to the C_{70} molecules. We emphasize that the enhanced charge transfer exists because the K ions "solvate" the C_{70} molecules.

charge state as arising from K saturation of the C_{70} molecule. The K-C_{70} atomic and molecular arrangements are then very different from those of an ordered fulleride crystal or an adsorbate on a rigid surface. The increased number of electrons that can be transferred to C_{70} compared to C_{60} might reflect the larger molecule size.

IV. SUMMARY

This paper has focused on the K-C_{70} system, defining the phase diagram and examining the electronic properties of the different phases. We have discussed phase stabilization at low doping, the structures that form upon higher doping, and the means that they can be examined spectroscopically. We have noted the importance of electron correlation and crystal symmetry in determining the valence-band structures. Comparison with the fullerides of C_{60} have shown common features that are rationalized via subtle changes in the Gibbs free energies of the respective phases. Logical continuations of this work will emphasize pressure-dependent studies of C_{70} to explore phase stabilization, diffraction investigations to determine the crystal symmetries, and studies of the Rb and Cs fullerides of C_{70}.

Note added in proof. A recent article by Kobayashi *et al.*[40] reports x-ray diffraction results for K_xC_{70}. They find the first doped phase to have the same structure as the starting material (fcc or rhombohedral). This is consistent with the K_1C_{70} phase reported here. The bct and bcc phases reported in Ref. 40 are likely to correspond to K_4C_{70} and K_6C_{70} as described here. While the "saturation-doped," fcc K_9C_{70} phase of Ref. 40 was not obtained under our reaction conditions, its existence is not inconsistent with our phase diagram for compounds with $x < 6$.

ACKNOWLEDGMENTS

This work was supported by the National Science Foundation. M.K. appreciates support by the German Academic Exchange Service (DAAD), and D.M.P. acknowledges partial support by the University of Minnesota Graduate School. Purified C_{70} was generously provided by R. E. Smalley and L. P. F. Chibante. Helpful discussions with P. J. Benning and F. Stepniak are gratefully acknowledged.

*Permanent address: Kernforschungszentrum Karlsruhe, Institut fur Nukleare Festkörperphysik, Postfach 3640, D-76021 Karlsruhe, Germany.

[1]See, for example, the review by J. H. Weaver and D. M. Poirier, in *Fullerene Fundamentals,* edited by H. Ehrenreich and F. Spaepen, Solid State Physics Vol. 48 (Academic Press, New York, in press), Chap. 1, other reviews in that volume, and extensive citations therein. See also A. F. Hebard, Ann. Rev. Mater. Sci. **23**, 159 (1993).

[2]R. C. Haddon *et al.*, Nature **350**, 320 (1991).

[3]T. Takahashi *et al.*, Physica C **190**, 205 (1992).

[4]P. J. Benning, D. M. Poirier, T. R. Ohno, Y. Chen, M. B. Jost, F. Stepniak, G. H. Kroll, J. H. Weaver, J. Fure, and R. E. Smalley, Phys. Rev. B **45**, 6899 (1992).

[5]E. Sohmen and J. Fink, Phys. Rev. B **47**, 14 532 (1993).

[6]K. Imaeda, K. Yakushi, H. Inokuchi, K. Kikuchi, I. Ikemoto, S. Suzuki, and Y. Achiba, Solid State Commun. **84**, 1019 (1992).

[7]M. Tomita, T. Hayashi, P. Gaskell, T. Maruno, and T. Tanaka, Appl. Phys. Lett. **61**, 1171 (1992).

[8]M. A. Verheijen, H. Meekes, G. Meijer, P. Bennema, J. L. de Boer, S. van Smaalen, G. van Tendeloo, S. Amelinckx, S. Muot, and J. van Landuyt, Chem. Phys. **166**, 287 (1992).

[9]G. B. M. Vaughan *et al.*, Science **254**, 1350 (1991).

[10]D. M. Poirier, T. R. Ohno, G. H. Kroll, P. J. Benning, F. Stepniak, J. H. Weaver, L. P. F. Chibante, and R. E. Smalley, Phys. Rev. B **47**, 9870 (1993).

[11]D. M. Poirier and J. H. Weaver, Phys. Rev. B **47**, 10 959 (1993).

[12]T. Yildirim, O. Zhou, J. E. Fischer, N. Bykovetz, R. A. Strongin, M. A. Chichy, A. B. Smith III, C. L. Lin, and R. Jelinek, Nature **360**, 568 (1992).

[13]A. R. Kortan, N. Kopylov, S. Glarum, E. M. Gyorgy, A .P. Ramirez, R. M. Fleming, F. A. Thiel, and R. C. Haddon, Nature **355**, 529 (1992).

[14]Y. Chen, D. M. Poirier, M. B. Jost, C. Gu, T. R. Ohno, J. L. Martins, J. H. Weaver, L. P. F. Chibante, and R. E. Smalley, Phys. Rev. B **46**, 7961 (1992).

[15]A. R. Kortan, N. Kopylov, S. Glarum, E. M. Gyorgy, A. P. Ramirez, R. M. Fleming, O. Zhou, F. A. Thiel, P. L. Trevor, and R. C. Haddon, Nature **360**, 566 (1992).

[16]M. Knupfer, F. Stepniak, and J. H. Weaver, Phys. Rev. B (to be published).

[17]Y. Z. Li, J. C. Patrin, M. Chander, J. H. Weaver, K. Kikuchi, and Y. Achiba, Phys. Rev. B **47**, 10 867 (1993).

[18]M. Knupfer, D. M. Poirier, and J. H. Weaver, Phys. Rev. B **49**, 2281 (1994).

[19]I. Elliott, C. Doyle, and J. D. Andrade, J. Electron Spectrosc. Relat. Phenom. **28**, 303 (1983).

[20]Discussions of the microstructures associated with a eutectoid transformation can be found in any introductory materials science text.

[21]Y. B. Zhao, D. M. Poirier, and J. H. Weaver, J. Phys. Chem. Solids (to be published).

[22]J. Baker, P. W. Fowler, P. Lazzaretti, M. Malagoli, and R. Zanasi, Chem. Phys. Lett. **184**, 182 (1991).

[23]D. M. Poirier, J. H. Weaver, K. Kikuchi, and Y. Achiba, Z. Phys. D **26**, 79 (1993).

[24]R. M. Fleming *et al.*, Nature **352**, 701 (1991).

[25]J. Winter and H. Kuzmany, Solid State Commun. **84**, 935 (1992).

[26]Q. Zhu, O. Zhou, J. E. Fischer, A. R. McGhie, W. J. Romanow, R. M. Strongin, M. A. Chichy, and A. B. Smith III, Phys. Rev. B **47**, 13 948 (1993).

[27]J. E. Fischer (private communication).

[28]D. M. Poirier, Appl. Phys. Lett. (to be published).

[29]J. L. Martins and N. Troullier, Phys. Rev. B **46**, 1766 (1992).

[30]G. A. Samara, J. E. Schirber, B. Morosin, L. V. Hansen, D. Loy, and A. P. Sylwester, Phys. Rev. Lett. **67**, 3136 (1991).

[31]M. Merkel, M. Knupfer, M. S. Golden, J. Fink, R. Seemann, and R. L. Johnson, Phys. Rev. B **47**, 11 470 (1993).

[32]W. Andreoni, F. Gygi, and M. Parrinello, Chem. Phys. Lett.

189, 241 (1992).

[33]T. Takahashi *et al.*, Phys. Rev. Lett. **68**, 1232 (1992); R. W. Lof *et al.*, *ibid.* **68**, 3924 (1992); C. Gu *et al.*, Phys. Rev. B **45**, 6348 (1992).

[34]P. J. Benning, F. Stepniak, and J. H. Weaver, Phys. Rev. B **48**, 9086 (1993).

[35]F. Stepniak, P. J. Benning, D. M. Poirer, and J. H. Weaver, Phys. Rev. B **48**, 1899 (1993).

[36]P. J. Benning, F. Stepniak, D. M. Poirier, J. L. Martins, J. H. Weaver, L. P. F. Chibante, and R. E. Smalley, Phys. Rev. B **47**, 13 843 (1993).

[37]S.-L. Ren, K. A. Wang, P. Zhou, Y. Wang, A. M. Rao, M. S. Meier, J. P. Selegue, and P. C. Eklund, Appl. Phys. Lett. **61**, 124 (1992).

[38]S. Satpathy, V. P. Antropov, O. K. Andersen, O. Jepsen, O. Gunnarsson, and A. I. Liechtenstein, Phys. Rev. B **46**, 1773 (1992).

[39]M. Knupfer, M. Merkel, M. S. Golden, J. Fink, O. Gunnarsson, and V. P. Antropov, Phys. Rev. B **47**, 13 944 (1993).

[40]M. Kobayashi, Y. Akahama, H. Kawamura, H. Shinohara, H. Sato, and Y. Saito, Phys. Rev. B **48**, 16 877 (1993).